# Supporting Information

## Chemicals and materials

AR grade powders of urea ($CH_4N_2O$, 99.5%), ethanol ($C_2H_6O$, 99.5%), Ammonia aqueous solution ($NH_4OH$, 28%), Formaldehyde solution (HCHO, 37%)，Titanium dioxide($TiO_2$), Silicon dioxide($SiO_2$) , active carbon(AC)， carbon nanotubes (CNT) and Rhodium (III) chloride ($RhCl_3 \cdot nH_2O$, 39%) were purchased from Aladdin Industrial Inc, China. Ammonia borane ($NH_3BH_3$, 97 %), and deuterium oxide ($D_2O$, 99.9 at%) were obtained from Beijing Innochem Science & Technology Co., LTD., China. All chemicals were used without further purification.

## Characterization

TEM images for each catalyst were obtained. The mean Rh particle size was calculated according to the statistical analysis of over 200 randomly selected particles based on the reported method[1]. The structure and morphology were characterized by a ZEISS Gemini 300 scanning electron microscope (SEM). Surface Areas were determined by BET measurements (Micromeritics ASAP2460). X-ray photoelectron spectrometry (XPS) analysis was carried out on a Thermo Scientific K-Alpha using an Al Kα source. Powder X-ray diffraction (XRD) was performed on Rigaku D/Max-2400X with Cu Ka radiation. The concentration of metals in the catalyst was measured via inductively coupled plasma optical emission spectrometry (ICP-OES, PerkinElmer Optima 8000 equipment).

**Calculation**

The TOF value was determined on the basis of the reported literature using the eq.(S1).

$$TOF = \frac{P_{atm}V_{H_2}/RT}{n_{Rh}t} \qquad \text{Eq. (S1)}$$

where Patm is the atmospheric pressure (101325 Pa), VH2 is the volume of generated hydrogen with 50% conversion of AB, R represents the ideal gas constant (8.314 J mol−1·K−1), T is the reaction temperature (K), nRh is the total mole number of Rh atoms in catalyst, and t is the reaction time for 50% conversion.

The KIE was determined on the basis of the reported literature using the Eq.(S2)

$$KIE = k_H / K_D \quad (S2)$$

where $k_H$ is the reaction constant of the reaction in $H_2O$, $k_D$ is the reaction constant of the reaction in $D_2O$.

**Mechanism for AB hydrolysis reaction**

$$NH_3BH_2OH + H_2O \rightarrow NH_3BH(OH)_2 + H_2 \qquad \text{(S3)}$$

$$NH_3BH(OH)_2 + H_2O \rightarrow NH_3BH(OH)_3 + H_2 \qquad \text{(S4)}$$

$$NH_3BH(OH)_3 + H_2O \rightarrow NH_4^+, B(OH)_4^- \qquad \text{(S5)}$$

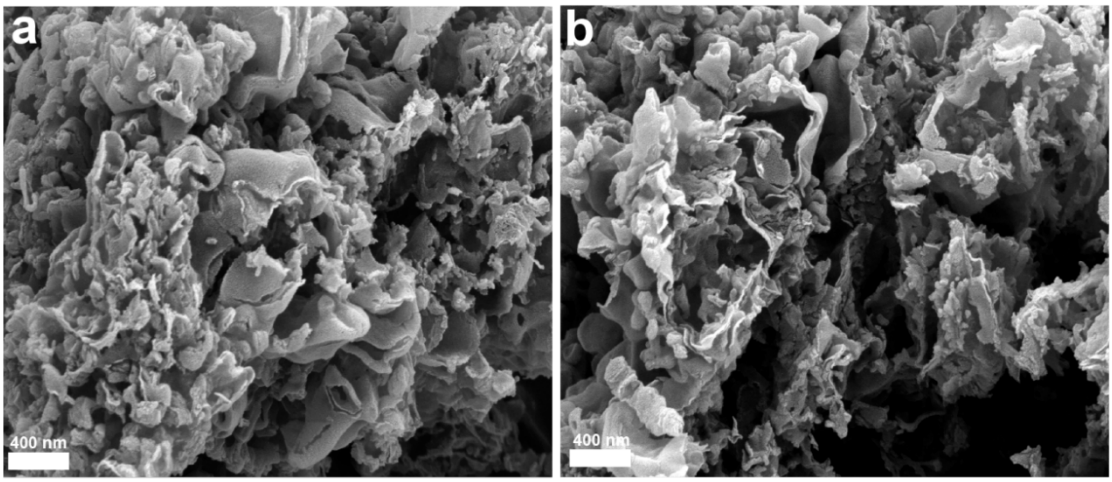


**Fig. S1.** (a, b) SEM images of h-NCNWs.

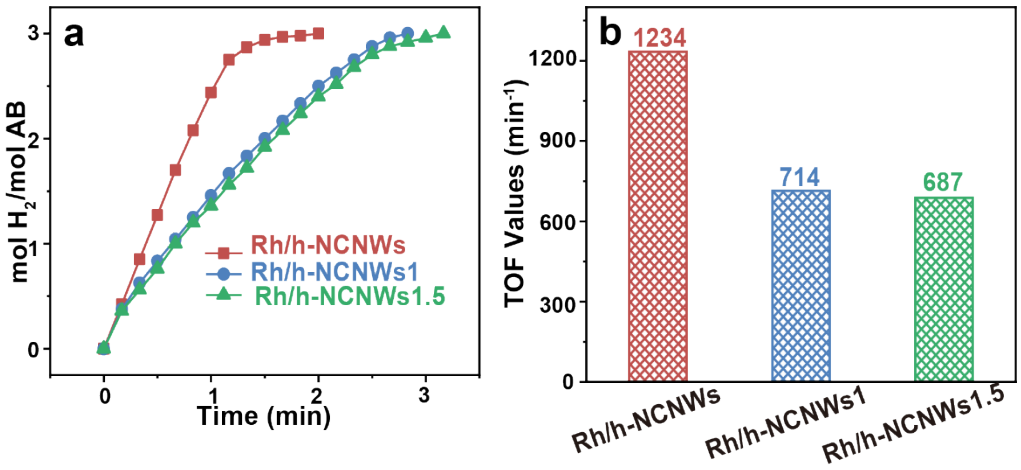


**Fig. S2.** (a) Time dependences of hydrogen production from hydrolytic dehydrogenation of AB at various catalysts. (b) The corresponding TOF values of (a).

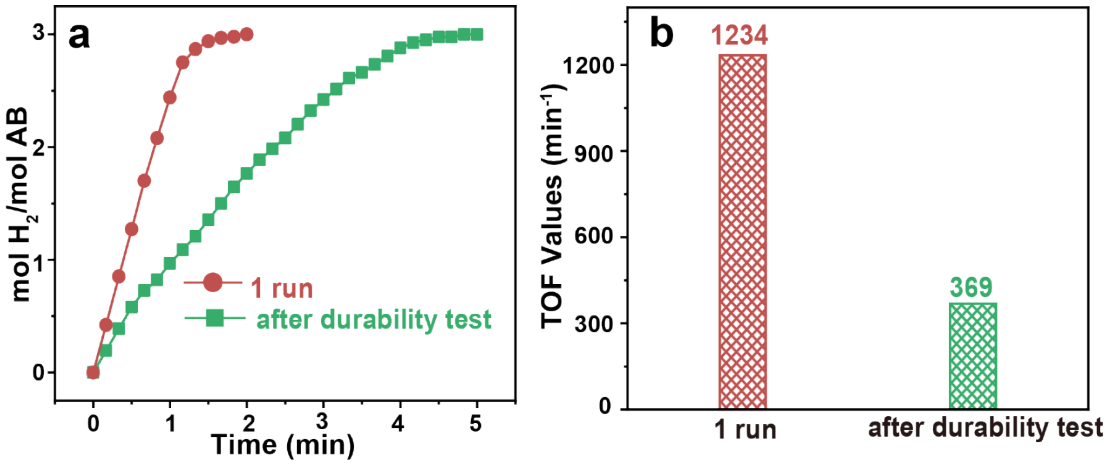


**Fig. S3.** (a) Hydrogen production plots of catalytic AB hydrolysis after the first and durable five times. (b) Corresponding TOF values of (a).

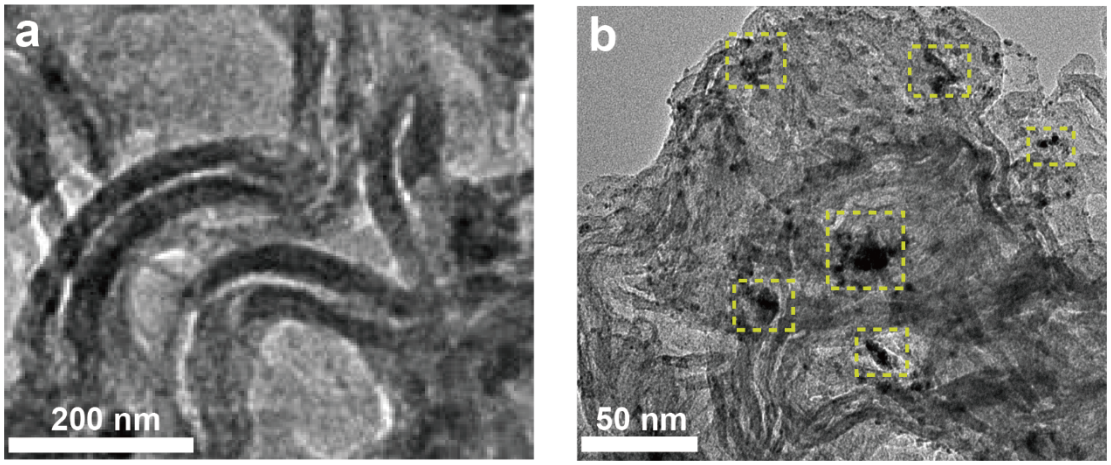


**Fig. S4.** (a-b) TEM images of Rh/h-NCNWs after durability test.

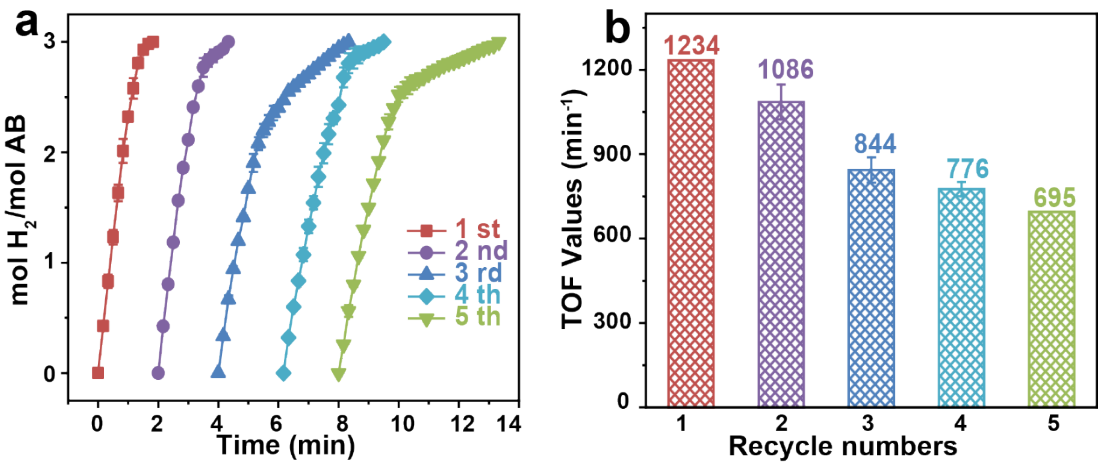


**Fig. S5.** (a) Recyclability tests for AB hydrolysis catalyzed by h-NCNWs. (b) The corresponding TOF values of (a).

**Table S1.** Binding energies of Rh/h-NCNWs.

| Name | Type | Binding Energies (eV) |
|---|---|---|
| C 1s | C-C/C=C | 284.8 |
| | C-N | 285.62 |
| | C-O | 286.8 |
| | C=N | 288.9 |
| | O=C-O | 291.0 |
| O 1s | Rh-O | 530.44 |
| | C=O | 531.8 |
| | O-H | 533.29 |
| Rh 3d | $Rh^0$ 3d5/2 | 307.8 |
| | $Rh^0$ 3d3/2 | 312.4 |
| | $Rh^{n+}$ 3d5/2 | 309.3 |
| | $Rh^{n+}$ 3d3/2 | 313.9 |
| N 1s | Pyridine N | 398.3 |
| | Pyrrole N | 400.7 |
| | Graphite N | 402.7 |
| | Oxide N | 404.9 |

**Table S2.** The ratios of different functional groups in Rh/h-NCNWs.

| Name | Type | Ratio (%) |
|---|---|---|
| C 1s | C-C/C=C | 47.2 |
| | C-N | 18.1 |
| | C-O | 16.4 |
| | C=N | 10.1 |
| | O=C-O | 8.2 |
| O 1s | Rh-O | 13.1 |
| | C=O | 54.3 |
| | O-H | 32.6 |
| Rh 3d | $Rh^0$ | 44.7 |
| | $Rh^{n+}$ | 55.3 |
| N 1s | Pyridinic N | 37.0 |
| | Pyrrole N | 45.7 |
| | Graphite N | 9.6 |
| | Oxide N | 7.7 |

**Table S3.** BET surface areas, pore volumes and pore diameters for the h-NCNWs and Rh/h-NCNWs.

| Sample | BET surface area ($m^2\ g^{-1}$) | Pore Volume ($cm^3\ g^{-1}$) | Pore size (nm) |
|---|---|---|---|
| h-NCNWs | 481.390 | 0.738 | 2.57 |
| Rh/h-NCNWs | 261.981 | 0.700 | 14.6 |

**Table S4.** Comparison with previous Rh NPs for AB hydrolysis.

| Catalysts | TOF ($Min^{-1}$) | Ea (kJ/mol) | T (°C) | Refs. |
|---|---|---|---|---|
| Rh/Ni@CN | 351 | 33.5 | 25.0 | [2] |
| Rh/AC | 180 | 39.9 | 25.0 | [3] |
| Rh/NPCC | 473.5 | 40.2 | 25.0 | [4] |
| Rh/C-SC | 336 | 37.1 | 25.0 | [5] |
| Rh/Ni@NCNTs | 959 | 41.0 | 25.0 | [6] |
| $Rh^0/nanoSiO_2$ | 112 | - | 25.0 | [7] |
| $Rh^0/nanoAl_2O_3$ | 112 | - | 25.0 | [7] |
| $Rh^0/HfO_2$ | 24 | - | 25.0 | [7] |
| $Rh^0$/CNT | 706 | 32 | 25.0 | [8] |
| Rh/PCNs | 513.2 | 46.5 | 25.0 | [9] |
| $Rh/Fe_3O_4$ | 273 | 58 | 25.0 | [10] |
| $Rh_{0.75}Co_{0.25}$/Ni@Ni-N-C | 223 | 28.63 | 25.0 | [11] |
| Rh/OPNC | 433 | 26.4 | 25.0 | [12] |
| $Rh^0/WO_3$ | 749 | 39 | 25.0 | [13] |
| $Rh/WO_{3-x}$ | 805 | 50.5 | 25.0 | [14] |
| $Rh@TiO_2$ | 334.1 | 28.3 | 25.0 | [15] |
| Rh/MXene | 288.4 | 54.2 | 25.0 | [16] |
| $Rh/Al_2O_3$CTAB | 186 | 44.8 | 25.0 | [17] |
| Rh/h-NCNWs | 1234 | 36.94 | 25.0 | This work |

## References


1. S. Galvagno, G. Capannelli, G. Neri, A. Donato and R. Pietropaolo, *Journal of Molecular Catalysis*, 1991, **64**, 237-246.
2. T. Sun, R. Lu, Y. Long, Q. Li, J. Wu and G. Fan, *International Journal of Hydrogen Energy*, 2021, **46**, 34229-34238.
3. S. Akbayrak, Z. Özçifçi and A. Tabak, *Journal of Colloid and Interface Science*, 2019, **546**, 324-332.
4. F. Zhong, Q. Wang, C. Xu, Y. Wang, B. Xu, Y. Zhang and G. Fan, *International Journal of Hydrogen Energy*, 2018, **43**, 22273-22280.
5. J. Chen, M. Hu, M. Ming, C. Xu, Y. Wang, Y. Zhang, J. Wu, D. Gao, J. Bi and G. Fan, *International Journal of Hydrogen Energy*, 2018, **43**, 2718-2725.
6. R. Lu, C. Xu, Z. Yang, L. Zhou, J. Wu, Y. Wang, Y. Zhang and G. Fan, *International Journal of Hydrogen Energy*, 2020, **45**, 1640-1648.
7. S. Akbayrak, Y. Tonbul and S. Özkar, *Applied Catalysis B: Environmental*, 2016, **198**, 162-170.
8. Q. Yao, Z.-H. Lu, Y. Jia, X. Chen and X. Liu, *International Journal of Hydrogen Energy*, 2015, **40**, 2207-2215.
9. H. Lin, C. Xu, Q. Wang, J. Wu, Y. Wang, Y. Zhang and G. Fan, *International Journal of Hydrogen Energy*, 2019, **44**, 21527-21535.
10. Y. Tonbul, S. Akbayrak and S. Özkar, *Journal of Colloid and Interface Science*, 2019, **553**, 581-587.
11. Z.-H. Zhang, L.-C. Liu, C.-X. Zhang, H.-L. Zhu and Y.-Q. Zheng, *International Journal of Hydrogen Energy*, 2023, **48**, 2640-2651.
12. Y. Peng, Y. He, Y. Wang, Y. Long and G. Fan, *Journal of Colloid and Interface Science*, 2021, **594**, 131-140.
13. S. Akbayrak, Y. Tonbul and S. Özkar, *International Journal of Hydrogen Energy*, 2021, **46**, 14259-14269.
14. X. Li, Y. Yan, Y. Jiang, X. Wu, S. Li, J. Huang, J. Li, Y. Lin, D. Yang and H. Zhang, *Nanoscale Advances*, 2019, **1**, 3941-3947.
15. H. Xu, W. Yu, J. Zhang, Z. Zhou, H. Zhang, H. Ge, G. Wang and Y. Qin, *Journal of Colloid and Interface Science*, 2022, **609**, 755-763.
16. Y. Karataş, T. Çetin, İ. N. Akkuş, Y. Akinay and M. Gülcan, *International Journal of Energy Research*, 2022, **46**, 11411-11423.
17. J. Chen, H. Cai and T. Zhao, *Molecular Catalysis*, 2022, **528**, 112518.